Acta Neurochir (2013) 155:1655–1660
DOI 10.1007/s00701-013-1780-3

CLINICAL ARTICLE - FUNCTIONAL

Stimulation sites in the subthalamic nucleus projected onto a mean 3-D atlas of the thalamus and basal ganglia

Johannes Sarnthein · Dominik Péus · Heide Baumann-Vogel · Christian R. Baumann · Oguzkan Sürücü

Received: 15 April 2013 / Accepted: 16 May 2013 / Published online: 1 June 2013

Abstract
Background In patients with severe forms of Parkinson's disease (PD), deep brain stimulation (DBS) commonly targets the subthalamic nucleus (STN). Recently, the mean 3-D Morel-Atlas of the basal ganglia and the thalamus was introduced. It combines information contained in histological data from ten post-mortem brains. We were interested whether the Morel-Atlas is applicable for the visualization of stimulation sites.
Methods In a consecutive PD patient series, we documented preoperative MRI planning, intraoperative target adjustment based on electrophysiological and neurological testing, and perioperative CT target reconstruction. The localization of the DBS electrodes and the optimal stimulation sites were projected onto the Morel-Atlas.
Results We included 20 patients (median age 62 years). The active contact had mean coordinates X_{lat}=±12.1 mm, Y_{ap}=−1.8 mm, Z_{vert}=−3.2 mm. There was a significant difference between the initially planned site and the coordinates of the postoperative active contact site (median 2.2 mm). The stimulation site was, on average, more anterior and more dorsal. The electrode contact used for optimal stimulation was found within the STN of the atlas in 38/40 (95 %) of implantations.
Conclusions The cluster of stimulation sites in individual patients—as deduced from preoperative MR, intraoperative electrophysiology and neurological testing—showed a high degree of congruence with the atlas. The mean 3D Morel Atlas is thus a useful tool for postoperative target visualization. This represents the first clinical evaluation of the recently created atlas.

Keywords Mean Atlas · 3D target visualisation · Parkinson's disease · Subthalamic nucleus · STN

J. Sarnthein (✉) · D. Péus · O. Sürücü
Klinik für Neurochirurgie, UniversitätsSpital Zürich,
Frauenklinikstrasse 10,
8091 Zürich, Switzerland
e-mail: Johannes.Sarnthein@usz.ch

H. Baumann-Vogel · C. R. Baumann
Klinik für Neurologie, UniversitätsSpital Zürich,
Frauenklinikstrasse 10,
8091 Zürich, Switzerland

Introduction

Deep brain stimulation (DBS) has become a widespread therapy for several neurological indications [4]. DBS has become a standard treatment for patients with advanced Parkinson's disease (PD). For many patients, a site within the subthalamic nucleus (STN) is chosen as an efficient target site to improve motor symptoms [3, 5, 6, 22].

In surgical practice, the anatomical location of the STN in individual PD patients is identified by several complementary approaches: 1) Preoperatively, MR images are scanned for a hypointense zone, which is caused by a susceptibility artefact due to iron enrichment in the subthalamic area [21]. This zone is used to identify the STN ("direct targeting" [2]). However, this zone does not necessarily correspond to the anatomical boundaries of the STN [12, 19]. 2) Intraoperatively, the location of the STN is verified by stepwise electrophysiological recording of neuronal activity with micro-electrodes. This measurement features the highest specificity and provides a spatial resolution in the submillimeter-scale along the electrode trajectory. Furthermore, electrophysiological recording shows a good correlation with the localization of STN in MR [16]. 3) Intraoperative neurological testing in the awake patient documents undesired side effects and clinical efficacy of the stimulation.

For postoperative documentation, stimulation sites in individuals can be projected on an atlas. There are a number of two-dimensional atlases that use the intercommissural line as a reference [11, 13, 17]. Since these atlases are based on

brain slices, the spatial resolution is highly anisotropic: very high within the slices and in the range of a millimeter in the direction perpendicular to the slices. Furthermore, due to the relatively small number of brains used for these atlases, a bias towards an individual brain might occur. To overcome these problems, the Yelnik group has constructed a three-dimensional atlas from one brain [23], which can be deformed to adapt to each individual patient [1]. In a different approach, a high-resolution, three-dimensional model of thalamic and subthalamic structures (3D-Morel Atlas) was recently constructed by combining information contained in histological data from ten post-mortem brains [10].

In the current study, we projected the implanted electrodes of a group of PD patients onto the 3D-Morel Atlas. We chose PD patients because the individual patient's STN can be localized on the basis of radiological, electrophysiological and neurological information. We use this information with the dual aim to visualize the optimal stimulation sites and to validate the applicability of the atlas for this purpose.

Methods

Patient inclusion criteria

We included all consecutive patients implanted with DBS electrodes in the STN for the treatment of PD in 2010 and 2011. Collection of personal data and scientific workup was approved by the institutional ethics review board (Kantonale Ethikkommission E-50/2009), and all patients gave their written informed consent. All surgeries were performed by the last author (OS).

Preoperative imaging and target planning

We followed a standard procedure known as "image based direct targeting" [2]. Preoperative MR images were obtained on a Philips Achieva 3T Scanner with the following two protocols: T1W_3D_TFE (FOV AP 240 mm RL 240 mm FH 160 mm, Voxel size 1 mm x 1 mm x 1 mm, Slice orientation transverse, Scan mode 3D, TE 6ms, TR 10ms, Flip angle 8°, Scan duration 4:51 min) and T2W_3D_VISTA (FOV AP 240 mm RL 240 mm FH 160 mm, Voxel size 1 mm×1 mm×1 mm, Slice orientation transverse, Scan mode 3D, TE 270ms, TR 2500ms, Flip angle 90°, Scan duration 7:42 min). The scans were fused using the StealthMerge algorithm on the Medtronic Framelink Stealth Station (www.medtronic.com). Then ventricular borders of the anterior and posterior commissures (AC, PC) were determined to obtain the mid-commissural point (MCP). Target planning was initiated at X_{lat}=±12 mm, Y_{ap}=−4 mm, Z_{vert}=−4 mm with respect to MCP, and then adapted to the hypointense zones associated with the nucleus ruber (RN), the substantia nigra (SN) and the STN in the MR images of the individual patient.

Intraoperative procedures

Electrode penetration to target was guided by a stereotactic frame (Riechert-Mundinger, www.inomed.de). We used up to five electrodes with a distance of 2 mm between electrodes (central, anterior, posterior, medial, lateral trajectory). By micro-electrode recording (MER), we performed electrophysiological recordings. An increase of MER background activity indicates the dorsal border of STN with submillimeter accuracy. Thereafter, during test stimulation through a macro-electrode, we performed a neurological testing of the cardinal symptoms of PD and documented side effects. On this basis, we determined the optimal site for stimulation. Then, the neurosurgeon implanted the definitive stimulation electrode (Medtronic Model 3389).

CT-based target reconstruction

After bilateral electrode implantation, we obtained a perioperative CT image to eliminate geometric image distortion (Siemens Sensation 64, Spiral CT without gantry tilt, axial scan reconstructed to slice thickness 1 mm). The CT image was fused with the preoperative MRI scans using the StealthMerge algorithm on the Medtronic Framelink Stealth Station. We then reconstructed the localization of the lowest contact of the stimulation electrode in AC-PC coordinates and the angle from the mid-sagittal plane (AMSP) and the angle from the axial plane (AFAP).

Clinical optimization of the stimulation site

After implantation, stimulation was started at the optimal contact determined during intraoperative neurological testing. In some patients, the stimulation was adapted to optimize clinical impact and to reduce side effects. The stimulation was optimized over a follow-up of at least 3 months. We documented the contact that was finally selected for stimulation.

The mean three-dimensional Morel Atlas

We present here a 3D version of the stereotactic Morel Atlas. A detailed description of the atlas can be found in [10, 13]. In brief, this atlas was constructed in the following way: 1) The structures of interest were analysed in three planes orthogonal to each other and oriented parallel or perpendicular to the reference stereotactic plane passing through the centers of AC and PC; 2) The delineation of structures based on multiarchitectonic criteria provides a high histological resolution; and 3) The slices were provided at small and regular

intervals. Furthermore, the atlas is based on histological data taken from ten postmortem brains, which reduces the bias towards a single brain. This results in a high-resolution, three-dimensional model of the anatomical structures of interest.

The STN of the 3D Morel Atlas compared with a recent MR study

In a recent study, the anatomy of the STN in eight post mortem tissue blocks was documented by high resolution MR with histological validation [12]. For the maximal distance in the axial plane from medial to lateral tip, these authors obtained a mean of x=12 mm, compared to 8.9 mm in the mean atlas used here. The maximal distance in axial plane between the anterior and posterior borders perpendicular to the width measurement was on average y=3.2 mm (3D Morel Atlas 5.5 mm). The maximal height obtained from the slices was on average z=6.6 mm (3D Morel Atlas 5.7 mm). The STN is oriented at approximately 40° to the midline (3D Morel Atlas 38°). This indicates that the mean STN volume used here has a more rounded shape, probably due to the fact of averaging over individual brains.

Projection of stimulation electrodes onto the 3D Morel Atlas

The stimulation electrode was projected onto to the atlas based on the localization of its lowest contact and of the angles AMSP and AFAP. The atlas and the electrode are represented by digital objects in .vtk format that are handled by the Parallel Visualization Application ParaView (www.paraview.org). The atlas is constructed such that all structures of the right hemisphere have been mirrored along the midsagittal plane. Consequently, in our application of the atlas, electrodes implanted in the right subthalamic region have been mirrored along the midsagittal plane to represent an electrode in the left subthalamic region. Since the locations of left and right STN are correlated in most patients, the left and right stimulation sites in the same patient are not statistically independent.

Inter-individual variability in lateral direction

For the projection of coordinates of individual patients onto a mean atlas, the inter-individual variability poses a major challenge. In our study, the atlas was not distorted so that the AC-PC distance remained fixed to 26 mm. For the lateral direction, there is strong correlation between ventricular width and the laterality of the hypointense zone reflecting the STN in MR images [8]. Therefore, to account for the variability in ventricular width of the patients' brain, the atlas was shifted in lateral direction for an alignment with the individual brain at the thalamo-ventricular border.

Results

Patient population

We included 20 patients with L-dopa responsive idiopathic PD (eight female, median age 62 years, range 42–76 years). All patients were implanted bilaterally, resulting in a total of 40 electrode implantations. Median AC-PC length was 25 mm (range 22.6-27.6 mm). The median width of the third ventricle was 4.3 mm (range 2.0 – 9.0 mm). Median duration of disease was 11.5 years (range 1–19 years). Akinesia and rigidity were present in all patients. Tremor was present in 17 patients; six of them had a tremor-dominant form of PD. The median score of Unified Parkinson's Disease Rating Scale (UPDRS part III) was 52 preoperatively (medication OFF) and improved to 15 postoperatively (medication ON, stimulation ON).

Intraoperative procedures

We tested all five electrode trajectories for six of the 40 electrode implantations (15 %). Four trajectories were tested in five (13 %), and three in 11 (28 %) implantations. In about half of the implantations, the number of trajectories tested was restricted to one (nine cases, 28 %) and two trajectories (nine cases, 28 %). Most frequently tested were central (all implantations, 100 %) and medial (28/40 implantations, 70 %) trajectories. Lateral (18/40, 45 %), anterior (14/40, 35 %), and posterior (9/40 23 %) trajectories were less frequently chosen. The use of trajectories was identical in left and right hemispheres in 12/20 patients (60 %), differed by one trajectory in 6/20 patients, and by three trajectories in 2/20 patients.

The anterior trajectory was tested in 14 cases. The microelectrode recording indicated only a short passage through STN (median 1.0 mm, range 0.0-6.5 mm). Neurological testing ensued in only three cases and gave optimal results in one patient only.

The final stimulation electrode (Medtronic Model 3389) was implanted through the central trajectory in 24/40 implantations (60 %), through the medial trajectory in 11/40 implantations (28 %), lateral and posterior two each (5 %) and anterior in one implantation (3 %).

Postoperative reconstruction of stimulation sites

The average coordinates of all 40 active stimulation sites were X_{lat}=12.1±1.3 mm (lateral), Y_{ap}=−1.8±1.4 mm (posterior of MCP), Z_{vert}=−3.2±1.3 mm (ventral of MCP) with AFAP=56° and AMSP=26°. The median Euclidian distance (bias) to the preoperatively determined target site was Δ=2.2 mm with the median deviations Δ X_{lat} =0.2 mm, Δ Y_{ap} =1.4 mm, Δ Z_{vert} =0.7 mm. Thus, the optimal stimulation site, which was determined in postoperative neurological testing, was more dorsal than planned preoperatively. Constrained by the angle

of the electrode trajectory, the optimal site was also more anterior than planned preoperatively.

Projection of electrodes and optimal stimulation sites onto the atlas

Figure 1A shows the atlas and a reconstructed electrode as viewed from anterior. In this penetration, the electrode enters the STN from antero-lateral at its dorso-lateral border in the plane of the STN and exits ventrally.

We finally computed coordinates of the optimal stimulation site as assessed by postoperative clinical testing. The sites are represented in Fig. 2 for all 40 penetrations. While the stimulating pole of the electrode has diameter 1.27 mm and length 1.5 mm, we chose spheres of diameter 0.4 mm for better visibility. Of the 40 penetrations, 38 (95 %) showed the pole of optimal stimulation within or in direct contact with the atlas' STN (95 % confidence interval [83.1–99.4 %]). All stimulating poles (100 %) were within 2 mm from STN, so that stimulation would modulate STN activity at this distance [7]. The red cylinder in Fig. 2 depicts the mean coordinates of the optimal stimulation sites in the dorso-lateral STN.

Discussion

Inter-individual variability and the mean atlas

This study describes the mapping of anatomical information of a group of 20 individual patient brains onto an atlas derived from a group of ten brains. The variability in the 40 brain hemispheres is accounted for at three levels. First, in the most important step ("direct targeting" [2]), we set the target into the hypointense zone in MR, which roughly corresponds to the STN [12]. This target coordinate was then adjusted on the basis of micro-electrode recording on one hand and neurological testing on the other hand. We finally reconstructed the coordinate of the sites of optimal stimulation based on postoperative follow-up examinations at least 3 months after surgery. Therefore, the individual stimulation sites contain anatomical information on the individual patient's brain hemisphere. Over all patients, we obtain a distribution of optimal stimulation sites (Fig. 2). The distribution is a cluster that is narrow compared to the extent of the STN.

The improvement in UPDRS was not related to the optimal stimulation site being situated within or outside the atlas' STN. We therefore assume that the deviation from the atlas' STN is not due to suboptimal surgical procedures,

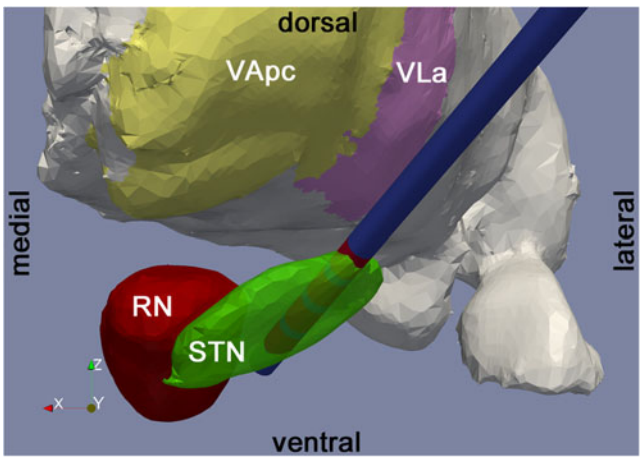

Fig. 1 Projections of the quadripolar electrode onto the atlas. View of an implanted electrode from anterior. Optimal stimulation was at the second most dorsal contact. Electrode shaft (blue) and stimulation contacts (red). Subthalamic Nucleus (STN, transparent green); Red Nucleus (red); Thalamus (gray) with thalamic nuclei: Ventral Anterior parvocellular division (VApc), Ventral Lateral anterior division (VLa)

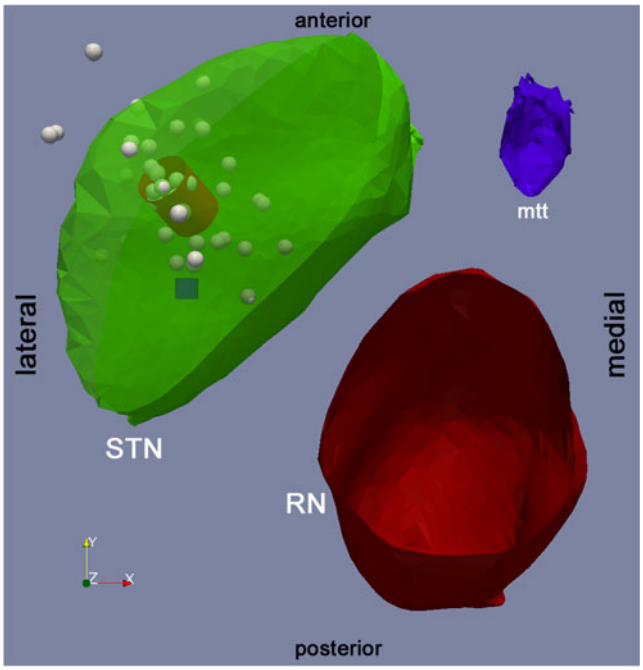

Fig. 2 Sites of optimal stimulation as determined in postoperative clinical practice. View on the axial plane. Subthalamic Nucleus (STN, transparent green); Red Nucleus (red); Mamillothalamic tract (blue) are clipped at $Z_{vert}=-4$ mm. All structures are mirrored to be depicted on the left hemisphere. Since the location of left and right STN are, in general, highly correlated, the left and right stimulation sites in the same patient are not statistically independent. The cube is positioned at the site where target planning was initiated ($X_{lat}=\pm12$ mm, $Y_{ap}=-4$ mm, $Z_{vert}=-4$ mm). Each sphere depicts the center of the optimal contact chosen for stimulation in individual patients before correction for ventricular width. The spheres are small (diameter=0.4 mm) for better visibility. The red cylinder is centered on the mean of the coordinates of the optimal stimulation site ($X_{lat}=\pm12.1$ mm, $Y_{ap}=-1.7$ mm, $Z_{vert}=-2.8$ mm) and oriented along the mean angles AFAP=56° and AMSP=26°. The dimensions of the cylinder correspond to that of a pole of Medtronic Model 3389 electrode (diameter 1.27 mm, height 1.5 mm)

but reflects the individual variability of the patients, be it in anatomy, age, disease duration or preoperative response to levodopa [9].

Adaptation of the mean atlas to landmarks

Apart from MCP, which is used to align the atlas with the patient's brain, there are a number of landmarks, that are known to correlate with selected features of the STN [8]. On this basis, the Yelnik Atlas [23] is deformed to adapt to each individual patient brain [1]. However, the correlation with most landmarks is rather low [8] and each deformation of the atlas introduces a new variable that must be justified. We have therefore restricted ourselves to the parameter "ventricular width", which is readily available and shows the highest correlation (0.73) with STN laterality [8]. We adjusted for the ventricular width of the patients to normalize the laterality of the STN.

Limitations in targeting, electrode placement and reconstruction

There are several sources of error that may affect the accuracy of the electrode placement and reconstruction. 1) Images from 3T MRI suffer from spatial distortions that may vary from patient to patient, and which we did not correct for. 2) The hypointense zone in MRI does not tightly correspond to the STN [12, 19]. 3) There are mechanical tolerances in the adjustment of the stereotactic frame. 4) We do not account for distortions of local tissue in the target area due to the insertion of electrodes. 5) The final stimulation electrode is inserted through an empty trajectory under visual inspection of x-ray images. This procedure may be affected by brain shift due to mechanical strain and/or loss of cerebrospinal fluid. The deviation between MR-target and reconstructed site may thus be maximal during the perioperative CT and may diminish as cerebrospinal fluid is replenished. 6) The typical error in CT-MR image fusion by the StealthMerge algorithm amounts to 1.2 mm [15]. 7) Identification of the electrode tip on volumetric CT scans has a spatial resolution that is limited by the distance between CT slices. 8) Mirroring all sites on the left hemisphere neglects that in most patients the geometry of left and right hemisphere is correlated: The difference between hemispheres in one patient (intra-individual variability) is smaller than the differences between patients (inter-individual variability).

Applicability of the mean atlas for target visualization in STN

The 3D-Morel Atlas uses the mean to represent the distribution of anatomical characteristics of the STN in ten brains. Interestingly, the overlap between the distribution of stimulation sites and the mean STN amounts to 95 % of sites. This amounts to a high degree of congruence between the atlas and information derived from image analysis of MR and CT, intraoperative electrophysiology, and neurological testing. The STN volume in the atlas thus provides a good representation of the STN in our patients, even though we have adapted only for ventricular width. The accuracy is certainly not sufficient to advocate atlas-based "indirect" targeting. But all current approaches to reconstruct stimulation sites show a more or less wide distribution [14, 18, 20, 23]. Our finding of the median of the optimal stimulation sites in the dorso-lateral STN agrees with reports that stimulation in the dorso-lateral STN [5, 22] improves motor symptoms in PD patients.

Conclusions

The cluster of individual stimulation sites—as deduced from preoperative MR, intraoperative electrophysiology and neurological testing in PD patients—showed a high degree of congruence with the atlas. Even with limited adaptation to the individual patient's brain, the mean 3D Morel Atlas is thus a useful tool for postoperative visualization of the stimulation electrode with respect to STN as the target. This represents the first clinical evaluation of the recently created atlas.

Conflict of interest None.

References

1. Bardinet E, Bhattacharjee M, Dormont D, Pidoux B, Malandain G, Schupbach M, Ayache N, Cornu P, Agid Y, Yelnik J (2009) A three-dimensional histological atlas of the human basal ganglia. II. Atlas deformation strategy and evaluation in deep brain stimulation for Parkinson disease. J Neurosurg 110:208–219
2. Bejjani BP, Dormont D, Pidoux B, Yelnik J, Damier P, Arnulf I, Bonnet AM, Marsault C, Agid Y, Philippon J, Cornu P (2000) Bilateral subthalamic stimulation for Parkinson's disease by using three-dimensional stereotactic magnetic resonance imaging and electrophysiological guidance. J Neurosurg 92:615–625
3. Benabid AL, Chabardes S, Mitrofanis J, Pollak P (2009) Deep brain stimulation of the subthalamic nucleus for the treatment of Parkinson's disease. Lancet Neurol 8:67–81
4. Benabid AL, Torres N (2012) New targets for DBS. Parkinsonism Relat Disord 18(Suppl 1):S21–23
5. Benarroch EE (2008) Subthalamic nucleus and its connections: Anatomic substrate for the network effects of deep brain stimulation. Neurology 70:1991–1995
6. Bronstein JM, Tagliati M, Alterman RL, Lozano AM, Volkmann J, Stefani A, Horak FB, Okun MS, Foote KD, Krack P, Pahwa R, Henderson JM, Hariz MI, Bakay RA, Rezai A, Marks WJ Jr, Moro E, Vitek JL, Weaver FM, Gross RE, DeLong MR (2011) Deep brain stimulation for Parkinson disease: an expert consensus and review of key issues. Arch Neurol 68:165

7. Butson CR, Cooper SE, Henderson JM, McIntyre CC (2007) Patient-specific analysis of the volume of tissue activated during deep brain stimulation. NeuroImage 34:661–670
8. Daniluk S, GD K, Ellias SA, Novak P, Nazzaro JM (2010) Assessment of the variability in the anatomical position and size of the subthalamic nucleus among patients with advanced Parkinson's disease using magnetic resonance imaging. Acta Neurochir (Wien) 152:201–210, discussion 210
9. Kleiner-Fisman G, Herzog J, Fisman DN, Tamma F, Lyons KE, Pahwa R, Lang AE, Deuschl G (2006) Subthalamic nucleus deep brain stimulation: summary and meta-analysis of outcomes. Mov Disord 21(Suppl 14):S290–304
10. Krauth A, Blanc R, Poveda A, Jeanmonod D, Morel A, Szekely G (2010) A mean three-dimensional atlas of the human thalamus: generation from multiple histological data. NeuroImage 49:2053–2062
11. Mai J, Paxinos G, Voss T (2007) Atlas of the Human Brain. Elsevier Academic Press
12. Massey LA, Miranda MA, Zrinzo L, Al-Helli O, Parkes HG, Thornton JS, So PW, White MJ, Mancini L, Strand C, Holton JL, Hariz MI, Lees AJ, Revesz T, Yousry TA (2012) High resolution MR anatomy of the subthalamic nucleus: Imaging at 9.4T with histological validation. NeuroImage 59:2035–2044
13. Morel A (2007) Stereotactic Atlas of the Human Thalamus and Basal Ganglia. Informa New York
14. Nowinski WL, Belov D, Pollak P, Benabid AL (2005) Statistical analysis of 168 bilateral subthalamic nucleus implantations by means of the probabilistic functional atlas. Neurosurgery 57:319–330, discussion 319–330
15. O'Gorman RL, Jarosz JM, Samuel M, Clough C, Selway RP, Ashkan K (2009) CT/MR image fusion in the postoperative assessment of electrodes implanted for deep brain stimulation. Stereotact Funct Neurosurg 87:205–210
16. Patil PG, Conrad EC, Aldridge JW, Chenevert TL, Chou KL (2012) The anatomical and electrophysiological subthalamic nucleus visualized by 3-T magnetic resonance imaging. Neurosurgery 71:1089–1095, discussion 1095
17. Schaltenbrand G, Wahren W (1977) Atlas for Stereotaxy of the Human Brain. Georg Thieme Stuttgart
18. Schlaier J, Schoedel P, Lange M, Winkler J, Warnat J, Dorenbeck U, Brawanski A (2005) Reliability of atlas-derived coordinates in deep brain stimulation. Acta Neurochir (Wien) 147:1175–1180, discussion 1180
19. Schlaier JR, Habermeyer C, Warnat J, Lange M, Janzen A, Hochreiter A, Proescholdt M, Brawanski A, Fellner C (2011) Discrepancies between the MRI- and the electrophysiologically defined subthalamic nucleus. Acta Neurochir (Wien) 153:2307–2318
20. Schönecker T, Kupsch A, Kuhn AA, Schneider GH, Hoffmann KT (2009) Automated optimization of subcortical cerebral MR imaging-atlas coregistration for improved postoperative electrode localization in deep brain stimulation. AJNR Am J Neuroradiol 30:1914–1921
21. Starr PA, Christine CW, Theodosopoulos PV, Lindsey N, Byrd D, Mosley A, Marks WJ Jr (2002) Implantation of deep brain stimulators into the subthalamic nucleus: technical approach and magnetic resonance imaging-verified lead locations. J Neurosurg 97:370–387
22. Wodarg F, Herzog J, Reese R, Falk D, Pinsker MO, Steigerwald F, Jansen O, Deuschl G, Mehdorn HM, Volkmann J (2012) Stimulation site within the MRI-defined STN predicts postoperative motor outcome. Mov Disord 27:874–879
23. Yelnik J, Bardinet E, Dormont D, Malandain G, Ourselin S, Tande D, Karachi C, Ayache N, Cornu P, Agid Y (2007) A three-dimensional, histological and deformable atlas of the human basal ganglia. I. Atlas construction based on immunohistochemical and MRI data. NeuroImage 34:618–638